# Momentum Distribution Dynamics of a Tonks-Girardeau Gas: Bragg Reflections of a Quantum Many-Body Wave Packet

R. Pezer[1] and H. Buljan[2]

[1]*Faculty of Metallurgy, University of Zagreb, Aleja narodnih heroja 3, 44000 Sisak, Croatia*
[2]*Department of Physics, University of Zagreb, PP 332, Zagreb, Croatia*
(Received 22 November 2006; published 14 June 2007)

The momentum distribution (MD) dynamics of a Tonks-Girardeau (TG) gas is studied in the context of Bragg reflections of a many-body wave packet. We find strong suppression of a Bragg reflection peak for a large and dense TG wave packet; our observation illustrates the dependence of the MD on the interactions and wave function symmetry. The MD is calculated from the reduced single-particle density matrix (RSPDM). We develop a method for calculating the RSPDM of a TG gas, which is operative for a large number of particles, and does not depend on the external potential and the state of the system. The method is based on a formula expressing the RSPDM via a dynamically evolving single-particle basis.

The possibility of constraining atomic gases to one-dimensional (1D) geometries [1–3] has led to experimental realizations of exactly solvable 1D models describing interacting Bose gases [4,5]. At low temperatures, low linear densities, and strong repulsive effective interactions, these 1D atomic gases enter a Tonks-Girardeau (TG) regime [6–8], which is described by an exactly solvable model of 1D bosons with "impenetrable core" repulsive interactions [4]. Two recent experiments achieved the TG regime and observed the properties of a TG gas [2,3]. One particularly interesting aspect of these 1D systems is their nonequilibrium dynamics. A recent experiment studying nonequilibrium dynamics of a 1D interacting Bose gas (including the TG regime) has shown that its momentum distribution (MD) does not need to relax to thermodynamic equilibrium even after numerous collisions [9]. These experimental advances and the possibility of exactly solving the TG model [4,10] motivate us to study the MD of the dynamically evolving TG gas.

The TG model is exactly solvable via Fermi-Bose mapping, which relates the TG gas to a system of noninteracting spinless 1D fermions [4,10]. Many properties of the two systems such as the single-particle (SP) density [4,10] or the thermodynamic properties [11] are identical. However, quantum correlations contained within the reduced single-particle density matrix (RSPDM), or the MD of the TG gas $n_B(k)$, considerably differ from those of the ideal Fermi gas $n_F(k)$ [12–22]. Although the exact many-body wave function describing TG gas can be written in compact form [4,10], the calculation of the RSPDM and the momentum distribution is a difficult task [13–22]. In the stationary case, the RSPDM and $n_B(k)$ were studied for a TG gas on the ring [13,18] and in the harmonic confinement [14,15,17,18]. In the homogeneous case, the MD has a singularity at $k = 0$, $n_B(k) \propto k^{-1/2}$ [13], and slowly decaying tails $n_B(k) \propto k^{-4}$ [15]. In both the homogeneous and the harmonic case, the occupation of the leading

natural orbital (effective SP state) is $\propto \sqrt{N}$ for large $N$ [18]. An analytic approximation for MD of a TG gas in a box has been made by generalizing Haldane's harmonic-fluid approach [16].

In the time-dependent case, the RSPDM and MD of the TG gas were studied in a harmonic potential with the time-dependent frequency [21]; the dynamics was solved with a scaling transformation [21]. Irregular motion and the dynamics of the MD were studied numerically for different interaction strengths (up to the TG limit) in Ref. [19]; solutions for $N = 6$ bosons were presented. Several recent studies have addressed the dynamics of hard-core bosons (HCB) on the lattice [20,22]. Numerical studies of this model revealed a number of interesting results including fermionization of the MD during 1D free expansion [20], and the possibility of relaxation of this system to a steady state, which carries memory of the initial condition [22]. However, the behavior of the *discrete* HCB-lattice model is not equivalent to the TG bosons in a *continuous* potential [23]. A feasible numerical study of the RSPDM and related observables during motion in a continuous potential $V(x, t)$ demands an efficient method for the calculation of the RSPDM, independent of the external potential, the state of the system, and operative for a larger number of particles.

Here we study dynamics of the momentum distribution, the RSPDM, natural orbitals (NOs), their occupancies, and entropy for a TG gas in a continuous potential. The results of the Letter are twofold: First, we develop an efficient method (with the desired aforementioned qualities) for calculating the RSPDM, which is based on a formula expressing the RSPDM via a dynamically evolving SP basis. Second, we employ the method to study Bragg reflections of a TG many-body wave packet in a periodic potential. A comparison of the TG bosonic ($n_B$) and non-interactiong fermionic ($n_F$) MDs illustrates the influence of interactions and wave function symmetry on this observ-

able. The MD of the ideal Fermi gas displays a beating peak at the edge of the Brillouin zone (BZ). In contrast, such a Bragg reflection peak is completely absent for a large and dense TG wave packet. As the TG wave packet reflects from the potential, it undergoes a rapid decrease of *spatial* coherence, characterized by the increase of entropy, and decrease of spatial correlations.

*The model.*—We consider dynamics of $N$ indistinguishable bosons in a 1D potential $V(x, t)$, which interact via impenetrable pointlike interactions [4]. The bosonic many-body wave function $\psi_B$ describing the system is related to a fermionic wave function $\psi_F$, which describes a system of $N$ noninteracting spinless fermions: $\psi_B(x_1, \ldots, x_N, t) = A(x_1, \ldots, x_N)\psi_F(x_1, \ldots, x_N, t)$, where $A = \Pi_{1 \leq i < j \leq N}\mathrm{sgn}(x_i - x_j)$ is a "unit antisymmetric function"; this is the famous Fermi-Bose mapping [4]. The dynamics of $\psi_F$ can be constructed from the Slater determinant $\psi_F = \det_{m, j=1}^{N}[\psi_m(x_j, t)]/\sqrt{N!}$, where $\psi_m(x, t)$ denote $N$ orthonormal SP wave functions obeying [10]

$$i\hbar \frac{\partial \psi_m}{\partial t} = \left[ -\frac{\hbar^2}{2m}\frac{\partial^2}{\partial x^2} + V(x, t) \right]\psi_m(x, t); \quad (1)$$

$m = 1, \ldots, N$. The TG wave function is $\psi_B = A(x_1, \ldots, x_N)\det_{m,j=1}^{N}[\psi_m(x_j, t)]/\sqrt{N!}$.

The RSPDM of the TG system, $\rho_B(x, y, t) = N \int dx_2 \ldots dx_N \psi_B^*(x, x_2, \ldots, x_N, t)\psi_B(y, x_2, \ldots, x_N, t)$, furnishes the expectation values of SP observables such as the position density $\rho_B(x, x, t)$, or momentum distribution $n_B(k, t) = (2\pi)^{-1}\int dx dy e^{ik(x-y)}\rho_B(x, y, t)$ [13]. The NOs $\phi_i(x, t)$ of the TG system, obtained as eigenfunctions of the RSPDM $\int dx \rho_B(x, y, t)\phi_i(x, t) = \lambda_i(t)\phi_i(y, t)$, $i = 1, 2, \ldots$, represent effective SP states, while eigenvalues $\lambda_i(t)$ represent their occupancies [14]. The SP wave functions $\psi_m(x_j, t)$ are NOs of the fermionic system, with occupancy unity, because the fermionic RSPDM is $\rho_F(x, y, t) = \sum_{m=1}^{N}\psi_m^*(x, t)\psi_m(y, t)$ [14]. The MDs can be expressed via the Fourier transform of the NOs, $n_F(k, t) = \sum_{m=1}^{N}|\tilde{\psi}_m(k, t)|^2$ and $n_B(k, t) = \sum_{i=1}^{\infty}\lambda_i(t)|\tilde{\phi}_i(k, t)|^2$.

*The method.*—The RSPDM can be expressed in terms of the dynamically evolving SP basis:

$$\rho_B(x, y, t) = \sum_{i,j=1}^{N}\psi_i^*(x, t)A_{ij}(x, y, t)\psi_j(y, t). \quad (2)$$

The $N \times N$ matrix $\mathbf{A}(x, y, t) = \{A_{ij}(x, y, t)\}$ is

$$\mathbf{A}(x, y, t) = (\mathbf{P}^{-1})^T \det \mathbf{P}, \quad (3)$$

where the entries of the matrix $\mathbf{P}$ are $P_{ij}(x, y, t) = \delta_{ij} - 2 \int_x^y dx' \psi_i^*(x', t)\psi_j(x', t)$; we have assumed $x < y$ without loss of generality.

Derivation of formula (3) is as follows. Define permutations $(k_2 \ldots k_N) = P(1 \ldots i - 1 i + 1 \ldots N)$, $(l_2 \ldots l_N) = Q(1 \ldots j - 1 j + 1 \ldots N)$, and their signatures $\epsilon(P)$ and $\epsilon(Q)$. The definition of $\rho_B$ and Eq. (2) yield

$$A_{ij} = \frac{(-1)^{i+j}}{(N-1)!}\int \prod_{n=2}^{N}dx_n \mathrm{sgn}(x - x_n)\mathrm{sgn}(y - x_n)$$

$$\times \sum_P \epsilon(P)\psi_{k_2}^*(x_2)\ldots\psi_{k_N}^*(x_N)$$

$$\times \sum_Q \epsilon(Q)\psi_{l_2}(x_2)\ldots\psi_{l_N}(x_N) \quad (4)$$

$$= \frac{(-1)^{i+j}}{(N-1)!}\sum_{P,Q}\epsilon(P)\epsilon(Q)\prod_{n=2}^{N}P_{k_n,l_n} \quad (5)$$

$$= (-1)^{i+j}\det \mathbf{P}_{ij}, \quad (6)$$

where $\mathbf{P}_{ij}$ is a minor of matrix $\mathbf{P}$ obtained by crossing its $i$th row and $j$th column. Equation (5) is obtained after rearranging the product factors of Eq. (4), and formally performing the integrations $P_{k_n, l_n} = \delta_{k_n, l_n} - 2 \int_x^y dx' \psi_{k_n}^*(x', t)\psi_{l_n}(x', t)$. Equation (6) follows from the definition of a determinant [18]. For $\det \mathbf{P} \neq 0$, Eq. (3) follows from Eq. (6) and the formula for the matrix inverse via algebraic cofactors.

Formulas (2)–(6) enable efficient and *exact numerical* calculation of the RSPDM; for a given pair of points $(x, y)$, and SP wave functions $\psi_i$, one needs to calculate $N \times N$ matrix $\mathbf{P}$, its inverse and determinant, for which there are fast and accurate numerical procedures. The numerical calculation of $\rho_B$ for every pair of points can be parallelized, and optimized given the fact that $\mathbf{P}$ changes only slightly for two adjacent points on the numerical grid. Moreover, formula (3) may open the way to (approximative) analytical studies of the RSPDM for certain cases; e.g., for $x \approx y$, $\mathbf{A} \approx (1 - \mathrm{Tr}\mathbf{Q})\mathbf{1} + \mathbf{Q}^T$, where $\mathbf{Q} = \mathbf{1} - \mathbf{P}$, $|Q_{ij}| \ll 1$.

*Bragg reflections.*—The richness of the dynamics of ultracold Bose gases in optical lattices [24] motivate us to study the evolution of a quantum many-body wave packet in a continuous periodic potential $V_p(x) = V_p(x + D)$ (also referred to as the lattice); periodic boundary conditions are assumed ($x$ space is a ring of length $L = n_s D$). The gas (wave packet) is initially localized, and it is given a certain amount of momentum. During dynamics, the many-body wave packet will disperse on the ring. The dynamics of the TG momentum distribution $n_B$ is affected by the exchange of the momentum between the lattice and the gas, the many-body interactions, and the bosonic symmetry of the wave function. On the other side, the related fermionic momentum distribution $n_F$ is affected by the lattice and the Pauli exclusion principle. A comparison of the two MDs during evolution illustrates the influence of the interactions and wave function symmetry on this observable.

In our calculations we consider $^{87}$Rb atoms, $V_p(x) = V_0\cos^2(\pi x/D)$, $D = 391.5$ $\mu$m, $V_0 = 11.9$ peV, and $N = 25$ unless specified otherwise; $n_s = 52$. For concreteness, the initial condition is chosen as $\psi_m(x, 0) = u_m(x)e^{ik'x}$,

$m = 1, \ldots, N$, where $u_m$ is the $m$th SP eigenstate of the harmonic potential $V_h(x) = m\omega^2 x^2/2$, $\omega = 2\pi 316$ Hz; the many-body wave packet $\psi_B(x_1, \ldots, x_N, 0)$ corresponds to a ground state of the gas in harmonic confinement, with imparted momentum $k'$ per particle. Note that the initial expectation value of the SP momentum $k' = \int dk k n_B(k, 0)$ is exactly at the edge of the BZ: $k' = \pi/D$. Although such an excitation is nontrivial to prepare, the current level of experiments [1–3,9] strongly suggests that it is more than just a theoretical curiosity.

We emphasize that the expectation value of the SP momentum is identical (at all times) for TG bosons and noninteracting fermions, $\langle k \rangle_B = \int dk k n_B(k, t) = \int dk k n_F(k, t) = \langle k \rangle_F$. Nevertheless, their MDs show remarkable differences. Figure 1(a) shows $n_F$ in the initial stage of the evolution, and after long-time propagation (when the gas is dispersed over the ring). A sharp peak beating up-down at the edge of the first BZ $k = -\pi/D$ arises from Bragg reflections. The fermionic MD is $n_F(k, t) = \sum_{m=1}^{N} |\tilde{\psi}_m(k, t)|^2$; a few of the SP spectra $|\tilde{\psi}_m(k, t)|^2$ are initially overlapping the edge of the BZ at $\pi/D$; as the dynamics of $\tilde{\psi}_m(k, t)$ are uncoupled, the spectra $|\tilde{\psi}_m(k, t)|^2$ of those NOs display a beating Bragg reflection peak at $-\pi/D$ which is reflected onto $n_F(k, t)$. This is illustrated in Fig. 1(b) up displaying $\sum_{m=1}^{5} |\tilde{\psi}_m(k, t)|^2$ (dot-dashed line) for the five fermionic NOs closest to the edge of the BZ.

The initial bosonic momentum distribution $n_B(k, 0)$ has a much sharper peak than the fermionic distribution

$n_F(k, 0)$; the peak is located exactly at the edge of the BZ [see Fig. 1(b)]. From this one may erroneously conclude that there would be a sharp beating peak originating from Bragg reflections at $-\pi/D$. However, this signature of Bragg reflections is *absent*; this is illustrated in Fig. 1(c), which shows a contour plot of $n_B(k, t)$. The signature is absent both at the beginning of the motion, when the wave packet is still localized, and after it spreads over the ring. In the long time propagation $n_B$ collectively oscillates due to the momentum-exchange with the lattice ($\langle k \rangle_B = \langle k \rangle_F$), but the changes in its shape are small. Our simulation clearly depicts that when the momentum is being transferred by the lattice to the TG gas, it redistributes among bosons; this leads to a smooth MD without beating Bragg reflection peaks. Unlike the fermionic NOs, the leading bosonic NOs do not display Bragg reflection peaks due to strong (nonlinear) coupling arising from interactions. This is illustrated in the lower part of Fig. 1(b), displaying $\sum_{i=1}^{12} \lambda_i(t) |\tilde{\phi}_i(k, t)|^2$; the leading 12 NOs are chosen for better comparison with dot-dashed curve in the upper part of Fig. 1(b), because $\int dk \sum_{i=1}^{12} \lambda_i(t) |\tilde{\phi}_i(k, t)|^2 \approx \int dk \sum_{m=1}^{5} |\tilde{\psi}_m(k, t)|^2$.

However, Bragg reflection peaks can be obtained for a smaller density of the TG gas; Fig. 1(d) shows an identical numerical simulation but with $N = 3$ bosons. In this case, as bosons expand on the ring, $n_B(k, t)$ undergoes the fermionization discussed in Ref. [20], resulting in a beating peak at $k = -\pi/D$.

We gain further insight into many-body dynamics by observing the *spatial coherence* and occupancies $\lambda_i$ of the bosonic NOs. Initially, a few of the leading $\lambda_i$s are fairly large, but they rapidly decrease after the evolution begins [see Fig. 2(a)]; simultaneously, the number of NOs with
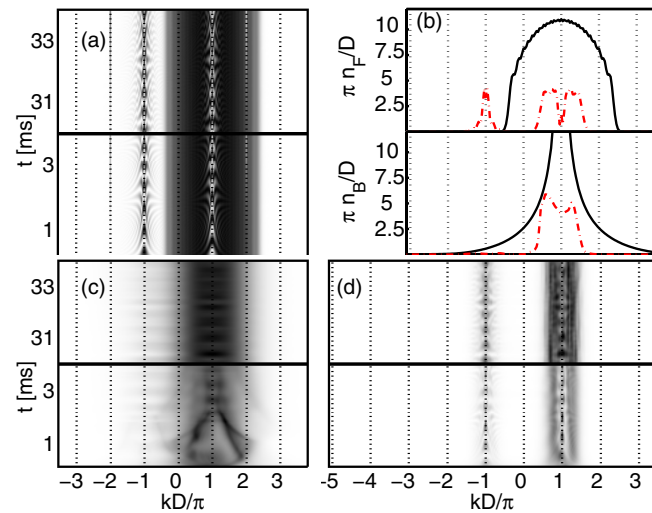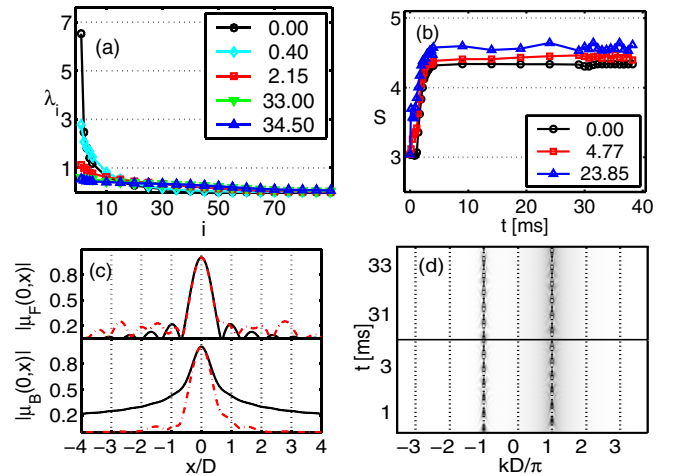


FIG. 1 (color online). Dynamics of MDs. (a) $n_F(k, t)$ in the initial stage of the evolution (lower), and after long-time propagation (upper); beating at $k = -\pi/D$ is a signature of Bragg reflections. (b) Initial MDs $n_F(k, 0)$ and $n_B(k, 0)$ for $N = 25$ bosons (solid lines); dot-dashed line depicts $\sum_{m=1}^{5} |\tilde{\psi}_m(k, t)|^2$ (upper), and $\sum_{i=1}^{12} \lambda_i(t) |\tilde{\phi}_i(k, t)|^2$ (lower) at $t = 34.5$ ms (see text). (c) $n_B(k, t)$ for $N = 25$ bosons in the initial evolution stage (lower), and after long-time propagation (upper); the signature of Bragg reflections at $k = -\pi/D$ is absent. (d) Dynamics of $n_B(k, t)$ for $N = 3$ bosons; there is beating at $k = -\pi/D$.



FIG. 2 (color online). Dynamics of bosonic NO occupations $\lambda_i$ and entropy $S$ for $N = 25$ bosons. (a) $\lambda_i(t)$ at times $t = 0, 0.40$, 2.15, 33, 34.5 ms; $V_0 = 11.9$ peV. (b) The entropy $S(t)$ for three different lattice depths $V_0 = 0, 4.77, 23.85$ peV. (c) $|\rho_F(0, x, t)|$ and $|\rho_B(0, x, t)|$ at $t = 0$ (solid line) and $t = 34.5$ ms (dot-dashed line); $V_0 = 11.9$ peV. (d) Dynamics of the MD for an ideal Bose gas. See text for details.

non-negligible occupations increases. This results in the increase of the entropy $S(t) = -\sum_i p_i \log p_i$, $p_i(t) = \lambda_i(t)/N$, which is illustrated in Fig. 2(b) for different lattice depths $V_0$. The entropy $S$ increases faster, and saturates at a higher value for a deeper lattice. Figure 2(c) shows bosonic (fermionic) degree of first-order spatial coherence [25] $\mu_B(x, x', t) = \rho_B(x, x', t)/\sqrt{\rho_B(x, x, t)\rho_B(x', x', t)}$, [$\mu_F(x, x', t)$, respectively] at $t = 0$ and $t = 34.5$ ms; $\mu_B$ ($\mu_F$) quantifies the fringe visibility that would be observed by interference of two spatially separated regions of the gas [26,27]. Note that in contrast to $\mu_B$, the fermionic correlations $\mu_F$ are not considerably changed during evolution. Figures 2(a)–2(c) illustrate *dynamical loss of the spatial coherence* of the TG wave packet, which is more rapid for deeper lattices. This results from the interplay of the many-body interactions and scattering from the lattice. Interactions couple bosonic NOs thereby providing a mechanism for the time change of their occupancies, while in a deeper lattice the initial wave packet excites a larger number of system's eigenstates leading to more irregular dynamics.

In order to elucidate the differences between the role of the interactions and statistics, we show MD dynamics of a noninteracting Bose gas [see Fig. 2(d)], but from the *identical* initial condition $\psi_B(x_1, \ldots, x_N, t = 0)$ as in Fig. 1(b) (lower part) and 1(c) (as if the interactions were suddenly turned off at $t = 0^+$). The bosonic NOs are uncoupled now (their populations do not change during evolution), which results in sharp Bragg reflection peaks.

Before closing, we note that dynamics of interacting Bose gases (including TG regime) may be related to incoherent light behavior in nonlinear and linear photonic structures [28,29], which motivate studies of the recently observed phenomena in optics [30] with Bose gases.

In conclusion, we have studied dynamics of the momentum distribution, RSPDM correlations, natural orbitals and their occupancies, and the entropy of the TG gas out of equilibrium. We have shown that the signature of Bragg reflections of the TG many-body wave packet may be considerably suppressed by the many-body interactions. We have introduced and employed a fast numerical method to calculate the RSPDM, which is applicable for versatile *continuous* potentials, and operative for a larger number of particles. Our results open the way for further studies of the RSPDM and related observables of the TG gas, both in the static and time-dependent cases.

[1] F. Schreck *et al.*, Phys. Rev. Lett. **87**, 080403 (2001); A. Görlitz *et al.*, Phys. Rev. Lett. **87**, 130402 (2001); M. Greiner *et al.*, Phys. Rev. Lett. **87**, 160405 (2001);

H. Moritz *et al.*, Phys. Rev. Lett. **91**, 250402 (2003); B. Laburthe Tolra *et al.*, Phys. Rev. Lett. **92**, 190401 (2004); T. Stöferle *et al.*, Phys. Rev. Lett. **92**, 130403 (2004).

[2] T. Kinoshita, T. Wenger, and D. S. Weiss, Science **305**, 1125 (2004).

[3] B. Paredes *et al.*, Nature (London) **429**, 277 (2004).

[4] M. Girardeau, J. Math. Phys. (N.Y.) **1**, 516 (1960).

[5] E. Lieb and W. Lineger, Phys. Rev. **130**, 1605 (1963); E. Lieb, Phys. Rev. **130**, 1616 (1963).

[6] M. Olshanii, Phys. Rev. Lett. **81**, 938 (1998).

[7] D. S. Petrov, G. V. Schlyapnikov, and J. T. M. Valraven, Phys. Rev. Lett. **85**, 3745 (2000).

[8] V. Dunjko, V. Lorent, and M. Olshanii, Phys. Rev. Lett. **86**, 5413 (2001).

[9] T. Kinoshita, T. Wenger, and D. S. Weiss, Nature (London) **440**, 900 (2006).

[10] M. D. Girardeau and E. M. Wright, Phys. Rev. Lett. **84**, 5691 (2000).

[11] K. K. Das, M. D. Girardeau, and E. M. Wright, Phys. Rev. Lett. **89**, 170404 (2002).

[12] M. D. Girardeau and E. M. Wright, Phys. Rev. Lett. **87**, 050403 (2001).

[13] A. Lenard, J. Math. Phys. (N.Y.) **5**, 930 (1964); H. G. Vaidya and C. A. Tracy, Phys. Rev. Lett. **42**, 3 (1979).

[14] M. D. Girardeau, E. M. Wright, and J. M. Triscari, Phys. Rev. A **63**, 033601 (2001); G. J. Lapeyre, M. D. Girardeau, and E. M. Wright, Phys. Rev. A **66**, 023606 (2002).

[15] A. Minguzzi, P. Vignolo, and M. P. Tossi, Phys. Lett. A **294**, 222 (2002).

[16] M. A. Cazalilla, Europhys. Lett. **59**, 793 (2002).

[17] T. Papenbrock, Phys. Rev. A **67**, 041601 (2003).

[18] P. J. Forrester *et al.*, Phys. Rev. A **67**, 043607 (2003).

[19] G. P. Berman *et al.*, Phys. Rev. Lett. **92**, 030404 (2004).

[20] M. Rigol and A. Muramatsu, Phys. Rev. Lett. **94**, 240403 (2005); see M. Rigol and A. Muramatsu, Mod. Phys. Lett. B **19**, 861 (2005) for a review of this topic.

[21] A. Minguzzi and D. M. Gangardt, Phys. Rev. Lett. **94**, 240404 (2005).

[22] M. Rigol *et al.*, Phys. Rev. Lett. **98**, 050405 (2007); M. Rigol, A. Muramatsu, and M. Olshanii, Phys. Rev. A **74**, 053616 (2006).

[23] M. A. Cazalilla, Phys. Rev. A **70**, 041604(R) (2004).

[24] O. Morsch and M. Oberthaler, Rev. Mod. Phys. **78**, 179 (2006).

[25] M. Naraschewski and R. J. Glauber, Phys. Rev. A **59**, 4595 (1999).

[26] I. Bloch, T. W. Hänsch, and T. Esslinger, Nature (London) **403**, 166 (2000).

[27] M. D. Girardeau and E. M. Wright, Phys. Rev. Lett. **84**, 5239 (2000).

[28] H. Buljan *et al.*, Phys. Rev. A **74**, 043610 (2006).

[29] H. Buljan, M. Segev, and A. Vardi, Phys. Rev. Lett. **95**, 180401 (2005).

[30] O. Cohen *et al.*, Nature (London) **433**, 500 (2005); H. Buljan *et al.*, Phys. Rev. Lett. **92**, 223901 (2004); G. Bartal *et al.*, Phys. Rev. Lett. **94**, 163902 (2005).